NJC

Accepted Manuscript

This is an *Accepted Manuscript*, which has been through the Royal Society of Chemistry peer review process and has been accepted for publication.

Accepted Manuscripts are published online shortly after acceptance, before technical editing, formatting and proof reading. Using this free service, authors can make their results available to the community, in citable form, before we publish the edited article. We will replace this *Accepted Manuscript* with the edited and formatted *Advance Article* as soon as it is available.

You can find more information about *Accepted Manuscripts* in the Information for Authors.

Please note that technical editing may introduce minor changes to the text and/or graphics, which may alter content. The journal's standard Terms & Conditions and the Ethical guidelines still apply. In no event shall the Royal Society of Chemistry be held responsible for any errors or omissions in this *Accepted Manuscript* or any consequences arising from the use of any information it contains.

ROYAL SOCIETY OF CHEMISTRY

www.rsc.org/njc

Journal Name

RSCPublishing

ARTICLE

Hierarchical architectures of Co_3O_4 ultrafine nanowires grown on Co_3O_4 nanowires with fascinating electrochemical performance

Cite this: DOI: 10.1039/x0xx00000x

Received ooth January 2015,
Accepted ooth January 2015

DOI: 10.1039/x0xx00000x

www.rsc.org/

Lei An[a], Li Yu[b], Yunjiu Cao[a,c], Wenyao Li[a,d], Kaibing Xu[a], Tao Ji[a,c], Rujia Zou[a,e] and Junqing Hu*[a]

A facile method to synthesize hierarchical architectures of Co_3O_4 nanowires@Co_3O_4 ultrafine nanowires grown on Ni foam was developed here. The unique architectures consisting of numerous ultrafine Co_3O_4 nanowires (shell) well grown on the surface of an Co_3O_4 nanowire (core) delivered remarkable electrochemical performance with ultrahigh specific capacitance (1640 F g^{-1} at a current density of 2 mA cm^{-2}), superior rate capability (66% retention of the initial capacitance from 2 mA cm^{-2} to 50 mA cm^{-2}) and outstanding cycling stability (~ 99.03% retention of the initial capacitance after 10000 cycles). Such fascinating capacitive behaviors can make these hierarchical architectures of Co_3O_4 nanowires@Co_3O_4 ultrafine nanowires a promising electrode material in electrochemical application.

Introduction

Recent years, unremitting efforts have been contributed to the exploration of high-performance electrode materials for electrochemical capacitor (EC), one of the most effective and practical devices for electrochemical energy storage.[1-6] There are two kinds of supercapacitors based on different ways of charge storage: electrical double-layer capacitors (EDLCs), in which store charges via reversible ion absorption at electrode/electrolyte interface, and pseudocapacitors, in which charge is stored based on fast and reversible surface redox reactions taking place on electrode surfaces, demonstrating prominently higher specific capacitance than EDLCs.[7-10]

Among various electrode materials of supercapacitors, cobaltosic oxide (Co_3O_4) can be one of advanced electrode material due to its high theoretical capacitance (3560 F/g), low cost, controllable size and shape, high availability, and good corrosion resistance in alkaline solutions.[11-17] To achieve out-bound electrochemical performance, it is significant to possess more electroactive sites for faradic redox reaction and enhance the kinetics of electron and ion transport on electrodes and electrode-electrolyte interface. Recently, numerous nanostructured Co_3O_4 morphologies have been investigated to meet such requirement. i.e. nanoparticles,[18] dendrite-like nanostructures,[19] nanocubes,[20] and rhombic dodecahedral structures,[21] However, most of the reported literatures were usually focused on the enhancement of its absolute specific capacitance values, and little attention has been devoted to other attributes, such as, the improvement of high-rate capabilities, an important factor to enhance electrochemical performance of an electrode material. Severe capacitance degradations at high current densities were discovered in above-mentioned reports for Co_3O_4 material. The recession may be attributed to insufficient active material involved in redox reaction with the increase of current density.[22] It is reported the diffusion distance of electrolytes in electrodes is only ~ 20 nm and active materials over this value can make less contribution to the total capacitance during the charge/discharge process.[23] Thus, ultrafine nanowires with a diameter below 10 nm can be investigated for high-performance supercapacitor. Additionally, integrated architectures with core/shell or hierarchical nanostructures have been fabricated as hybrid supercapacitor electrodes and show good electrochemical properties as the core can offer an efficient way of transporting the ions or electrons, while the shell offers small voids for high ion accessibility.[24-26] Although hierarchical structures have been prepared from metal oxides, the controllable synthesis of a Co_3O_4 material with desirable hierarchical architecture possessing an ultrafine nanostructure and predominant electrochemical performance with high specific capacitance, superior rate capability and long lifespan simultaneously still remains a great challenge.

Herein, we have reported a facile effective hydrothermal method for the growth of hierarchical architectures of Co_3O_4 nanowires@Co_3O_4 ultrafine nanowires on Ni foam and investigated their electrochemical performance as an electrode material for supercapacitor by means of cyclic voltammetry, galvanostatic charge-discharge method and impedance

spectroscopy and compared the performance with those of conventional Co_3O_4 nanowires without ultrafine nanostructures. The hierarchical architectures of Co_3O_4 nanowires@ nanowires exhibited a high specific capacitance of 1640 F g^{-1} at 2 mA cm^{-2}, which is superior to 560 F g^{-1} of the conventional Co_3O_4 nanowires at the same current density. More importantly, this unique microstructures delivered an high specific capacitance (1083 F g^{-1}) at a current density as high as 50 mA cm^{-2}, a superior rate performance (~ 66% retention of the initial capacitance from 2 mA cm^{-2} to 50 mA cm^{-2}) and a long lifespan (~ 99.03% retention of the initial capacitance after 10000 cycles). Such intriguing capacitive behavior is ascribed to the unique core/shell hierarchical configuration with ultrafine nanostructures, leading Co_3O_4 nanowires@Co_3O_4 ultrafine nanowires to be a promising electrode material in electrochemical application.

Experimental Characterization

All the chemicals were of analytical grade and used without further purification.

Synthesis

All the chemicals were of analytical grade and used without further purification. Firstly, one segment of Ni foam (~ 3 cm × 1 cm) was carefully cleaned with 6 M HCl solution in an ultrasound bath for 20 min to remove a NiO layer from the surface, and then rinsed with deionized water and absolute ethanol several times until neutral. Secondly, 1 mmol of $Co(NO_3)_2 \cdot 6H_2O$ and 15 mmol of urea were dissolved in 40 mL of deionized water to form a homogeneous magenta solution. The solution and as pre-treated Ni foam were transferred into a 50 mL of Tefion-lined stainless-steel autoclave, which was sealed and maintained at 110 ℃ for 5 h. After being cooled down to room temperature, the products were collected and washed with deionized water and absolute ethanol several times, then vacuum dried at 60 ℃ for 4 h. Finally, the products were calcined at 350 ℃ in a normal N_2 atmosphere with a ramping rate of 1 ℃ min^{-1} for 2 h. Conventional Co_3O_4 nanowires were prepared according to a previous publication.[23]

Characterization

X-ray diffraction (XRD) patterns were carried out with D/max-2550 PC X-ray diffractometer (XRD; Rigaku, Cu-Kα radiation). The morphology of the materials was examined by a scanning electron microscope (SEM; S-4800) equipped with an energy dispersive X-ray spectrometer (EDX) and a transmission electron microscope (TEM; JEM-2100F). The mass of electrode materials was weighed on an XS analytical balance (Mettler Toledo; δ = 0.01 mg).

Electrochemical measurement

Electrochemical measurements were performed on an Autolab Electrochemical Workstation (PGSTAT302N) using a three electrode electrochemical cell and 2 M KOH as the electrolyte. The Ni-foam-supported electrode materials (~ 1 cm × 1 cm, ~ 1.18 and ~ 0.82 mg cm^{-2} for hierarchical Co_3O_4 nanowires@nanowires and conventional Co_3O_4 nanowires, respectively.) were used directly as the working electrode. A saturated calomel electrode (SCE) was used as the reference electrode and a platinum (Pt) sheet electrode was used as the counter electrode. All potentials were referred to the reference electrode. The specific capacitance and current density were calculated based on the mass of these electroactive materials.

Results and discussion

The Co-based intermediates are first obtained from the magenta hydrothermal reaction, and their morphology was characterized by SEM, with the results shown in Fig. S1. It can be clearly identified from Fig. S1a that the intermediates with a high density are uniformly distributed on Ni foam, forming an ordered array with an opened-up network. Higher-magnification SEM images shown in Fig. S1b clearly display that the internal nanowires directly grew on Ni foam along with the external multidirectional ultrafine nanowires grounded on the internal nanowires. XRD pattern (Fig. S2) shows that all the identified peaks can be assigned to cobalt carbonate hydroxide hydrate ($Co(CO_3)_{0.5} \cdot 0.11H_2O$) crystal (JCPDS card no. 48-0083).

Journal Name

RSCPublishing

ARTICLE

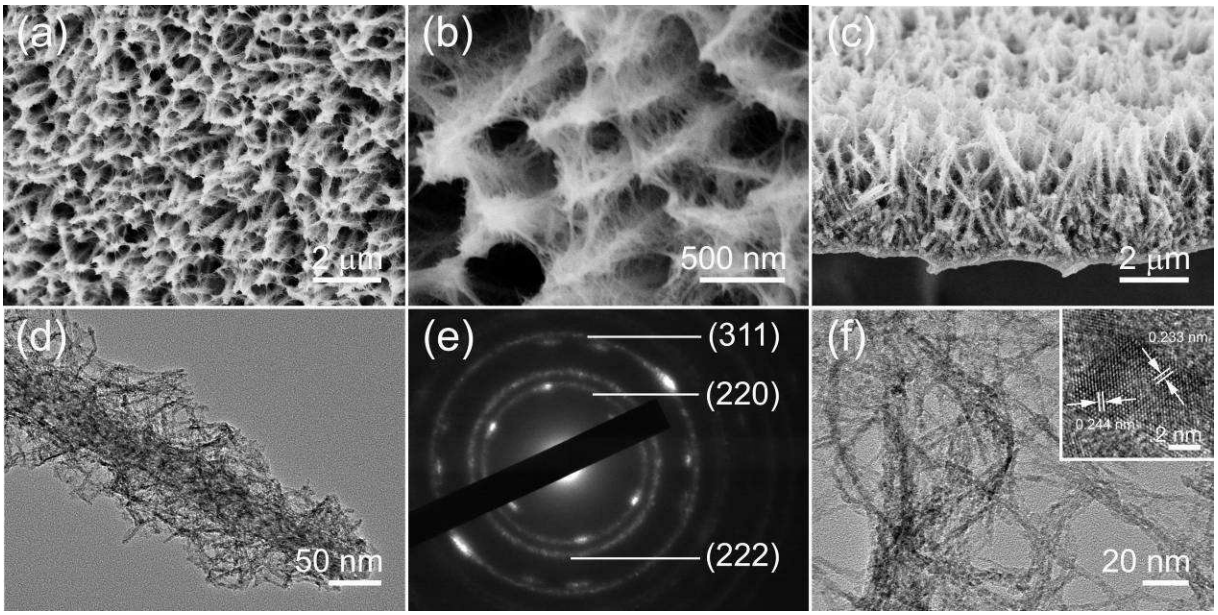

Fig. 1 (a) (b) Low and high magnification SEM images of the hierarchical Co_3O_4 nanowires@nanowires on Ni foam. (c) SEM image of Co_3O_4 nanowires@nanowires from the side view; (d) TEM image of the hierarchical Co_3O_4 nanowires@nanowires scraped off from Ni foam; (e) The corresponding SAED pattern of (d); (f) high-magnification TEM image of the Co_3O_4 ultrafine nanowires. The inset is the corresponding HRTEM image.

In order to obtain pure Co_3O_4 material, we subsequently thermally treated as-prepared $Co(CO_3)_{0.5}$•$0.11H_2O$ product at 350 ℃ for 2 h in a normal N_2 atmosphere. As seen from different magnification SEM images, Fig. 1a, b, the original morphology of the $Co(CO_3)_{0.5}$•$0.11H_2O$ products is kept perfectly, and the ultrafine nanowires still grown on the major nanowires, exhibiting a unique core/shell hierarchical feature with suitable rooms among neighbouring nanounits. Figure 1c shows the hierarchical microstructure arrays homogeneously aligned from the side view and their height is ~ 5 μm. Such unique hierarchical microstructures possessing more electroactive sites can improve electrolyte diffusion efficiency and increase electron transport when used as an electrode for supercapacitor, resulting promotion of electrochemical performance. Oppositely, the SEM image of conventional Co_3O_4 nanowires (Fig. S3) prepared according to previous publication [27] reveals crowded space among adjacent nanowires, which may render difficult diffusion of the electrolyte into the inner region.

The morphology and structure of the hierarchical nanowires@ultrafine nanowires are further elucidated by TEM. As shown in Fig. 1d-f, Fig. 1d shows the TEM image of the Co_3O_4 nanowires@nanowires samples scraped off from the Ni foam. Clearly, the internal nanowires were used as the backbone material, while the external ultrafine nanowires were grown on the backbone, which can agree with that of the preceding SEM images. The diameter of the internal nanowire is estimated to be about 50 nm. The corresponding selected-area electron diffraction (SAED) pattern (Fig. 1e) of the whole hierarchical microstructure shows well-defined diffraction rings, which correspond to the (222), (220) and (311) planes, demonstrating that the as-synthesized sample is polycrystalline. A high-magnification TEM image of the ultrafine nanowires, as shown in Fig. 1f, exhibits a diameter of ~ 2-3 nm. These ultrafine nanowires would accessible to the electrolyte highly and participate in the reversible faradic reaction adequately due to the presence of convenient diffusion paths. Besides, the corresponding HRTEM image (inset) reveals lattice fringes with d-spacings of 0.244 and 0.233 nm, corresponding to the distance of the (311) and (222) planes, respectively, of the Co_3O_4 crystal.

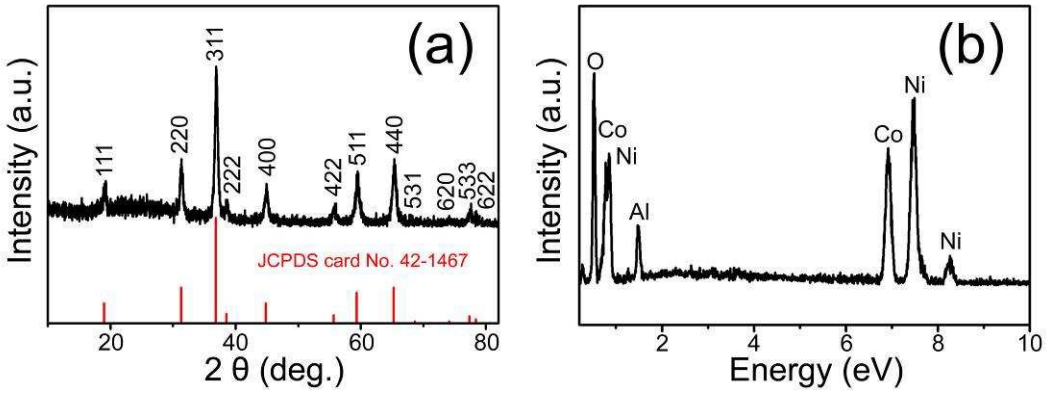

Fig. 2 (a) XRD patterns of the hierarchical Co_3O_4 nanowires@nanowires scraped off from the Ni foam. (b) The EDX spectrum of the Co_3O_4 nanowires@nanowires on the Ni foam.

In order to eliminate the strong impact of the Ni foam substrate on the XRD peak signals, the nanowires@nanowires powder was scratched from the Ni foam for XRD analysis. As indicated in Fig. 2a, the XRD pattern confirms that all the diffraction peaks can be indexed to Co_3O_4 phase (JCPDS no. 42-1467). The relatively high peak intensities indicate that the Co_3O_4 sample was of high crystallinity, which is consistent with the prior TEM results. In order to better understand the chemical composition of the as-prepared nanowires@nanowires, the energy dispersive X-ray (EDX) spectrometry characterization of the as-prepared nanowires@nanowire microstructures was also conducted. In Fig. 2b, it was found that the microstructure consist of Co, Ni, O, and Al elements, in which the Al peaks were derived from the aluminum platform and Ni signal comes from Ni foam, further indicating the formation of the Co_3O_4 crystal.

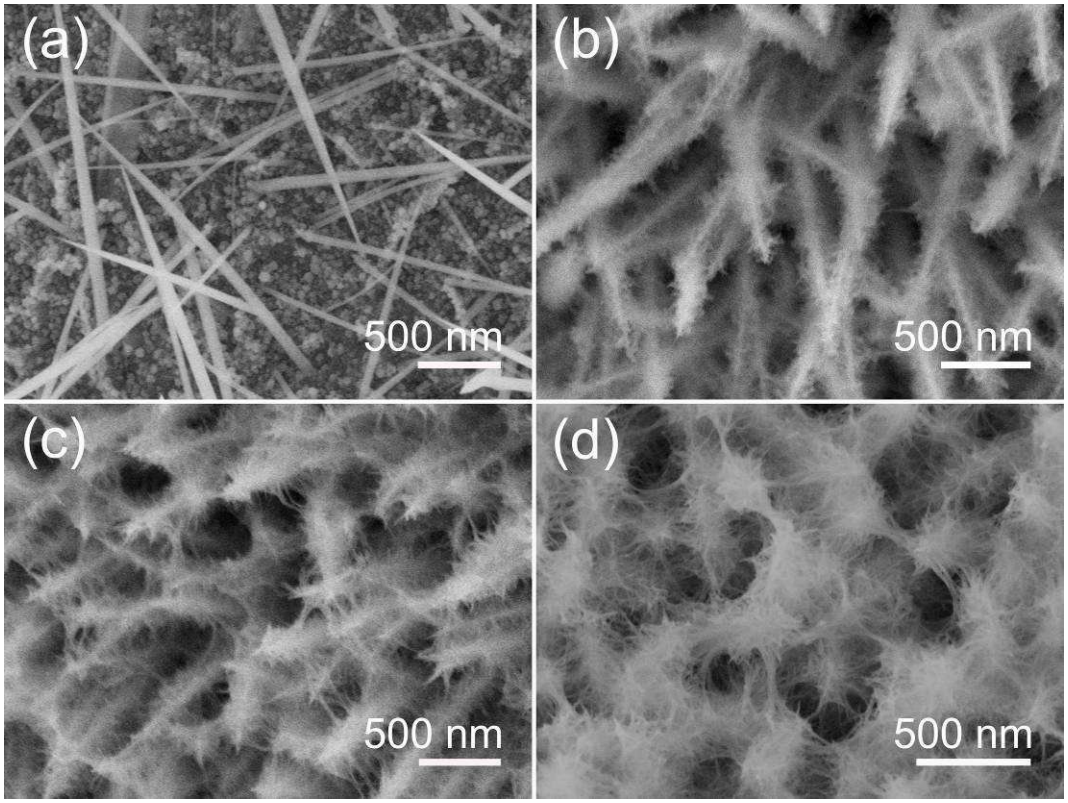

Fig. 3 SEM images of the hierarchical Co_3O_4 nanowires@nanowires grown via different reaction times: (a) 1 h, (b) 2 h, (c) 5 h, and (d) 14 h.

We next demonstrate the formation mechanism of our synthetic system via modifying the reaction time to reveal different reaction stages. Figs. 3a-d are the SEM images of the samples obtained at various growth times, indicating a transform of the structure and morphology (intermediate) to Co_3O_4 nanowire@nanowire arrays finally. After the initial 1 h reaction, many nanoparticles nucleated on the surface of the Ni foam and some nanowires grew based on these crystal nucleus, as shown in Fig. 3a. With the reaction time prolonging to 2 h, these crystal nucleus were developed into Co-based intermediate nanowires completely with a high density on the substrate (Fig. 3b). Meanwhile, many ultrafine and short nanowires appeared and grew on the surface of the backbone nanowires. With unremitting extending reaction time to 5h, these nanowires became

long and dense (Fig. 3c). It can be concluded that the backbone internal nanowires can gives birth to multiple directional ultrafine microstructure on the surface. These ultrafine microstructures are interconnected with each other, leading a unique core/shell hierarchical feature with rational interspaces among adjacent nanostructures. Further increasing the reaction time to 14 h, the nanowires got extremely dense and longer with deficient interspace (Fig. 3d), which may cause difficult diffusion of the electrolyte into the inner region when as an electrode. This evolution processes seems to be a similar circumstance found in other material systems. [28, 29]

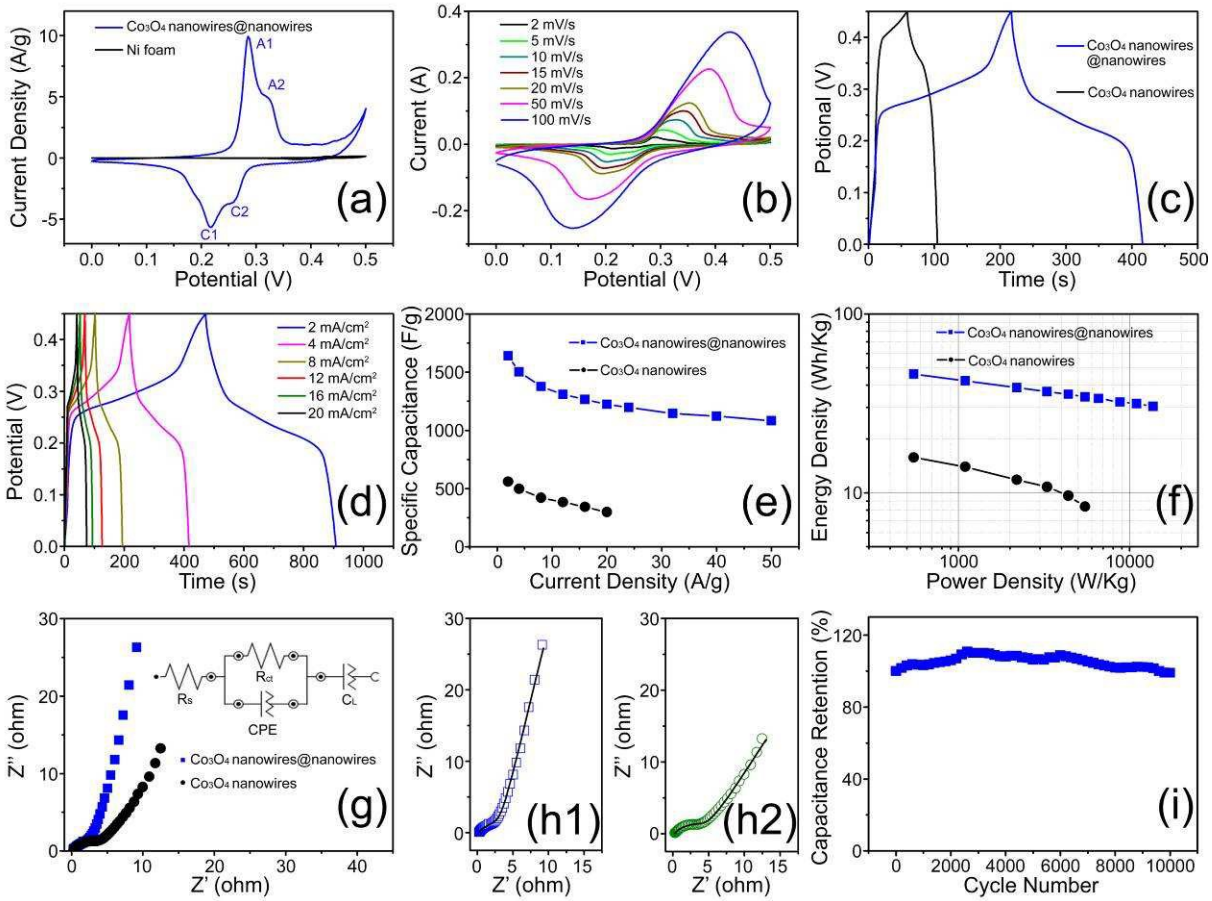

Fig. 4 (a) CV curves of the hierarchical Co_3O_4 nanowires@nanowires and **Ni foam** at a scan rate of 1 mV s^{-1}; (b) CV curves of the hierarchical Co_3O_4 nanowires@nanowires at different scan rates; (c) galvanostatic charge-discharge curves of the hierarchical Co_3O_4 nanowires@nanowires and conventional Co_3O_4 nanowires with a current density of 4 mA cm^{-1}; (d) galvanostatic charge-discharge curves of the hierarchical Co_3O_4 nanowires@nanowires at different current densities; (e) specific capacitance at different current densities, (f) Ragone plot (power density vs. energy density), (g) EIS spectra comparison, (h1) and (h2) fitting curves of the hierarchical Co_3O_4 nanowires@nanowires and conventional Co_3O_4 nanowires, respectively; (i) variation of specific capacitance with the cycle number at a scan rate of 50 mV s^{-1} of the hierarchical Co_3O_4 nanowires@nanowires.

The electrochemical tests were carried out in a three-electrode configuration using a Pt counter electrode and a SCE reference electrode in 2 M KOH aqueous electrolyte. Fig. 4a shows the CV curves of the Ni foam supported-Co_3O_4 nanowires@nanowires and pure Ni foam at a scan rate of 1 mV s^{-1}. Two pairs of well-defined redox peaks indicate good super-capacitive characteristics, similar to previous literatures of Co_3O_4 electrodes.[30-32] The first redox couple A1/C1 is ascribed to the conversion between Co_3O_4 and CoOOH, illustrated as follows: [33, 34]

$$Co_3O_4 + OH + H_2O \leftrightarrow 3CoOOH + e^- \quad (1)$$

The second redox peak of A2/C2 corresponds to the change between CoOOH and CoO_2, represented by the following reaction: [33, 34]

$$CoOOH + OH^- \leftrightarrow CoO_2 + H_2O + e^- \quad (2)$$

However, for the pure Ni foam as an electrode, the response current is relatively very weak, which can be negligible in contrast with that of as-prepared Co_3O_4 electrode. A contribution from the Ni foam to the total capacitance was ignored in the following discussion as the capacitance is proportional to the area directly within the enclosed area of CV curve. The CV behaviour of the hierarchical Co_3O_4 nanowires@nanowires changed as the scanning rate increasing from 1 mV s^{-1} to 100 mV s^{-1} (Fig. 4b). Two oxidation (A1 and A2) and reduction peaks (C1 and C2) merge with each other at higher scanning rate, resulting one oxidation and reduction peaks. Besides, the oxidation and reduction peaks shift continuously to higher and lower potentials, respectively, with a larger potential separation between the oxidation and the reduction peak, indicating remarkable faradic reversibility. A similar phenomenon was also discovered in the conventional Co_3O_4 nanowires (Shown in Fig. S4).

Galvanostatic charge-discharge measurements (CD) were also conducted on the hierarchical Co_3O_4 nanowires@nanowires at different current densities. Fig. 4c depicts the comparison of CD curves at a stable potential window between 0 and 0.45 V for the Co_3O_4 nanowires@nanowires and conventional Co_3O_4 nanowires electrodes at the same current density of 4 mA cm^{-2}. As respected, the Co_3O_4 nanowires@nanowire electrode reveals a much longer discharging time compared with that of the conventional Co_3O_4 nanowires. This means the as-synthesized hierarchical Co_3O_4 nanowires@nanowires demonstrate higher specific capacitance values than the conventional Co_3O_4 nanowires electrode. Further CD curves of the Co_3O_4 nanowires@nanowires electrode was recorded with various current densities ranging from 2 to 50 mA cm^{-2}, as shown in Fig. 4d and Fig. S5. However, it is obvious that all shapes of these CD curves are not strictly but approximately symmetric to their corresponding discharge counterparts, also indicating their good reversibility, which is consistent with the CV investigations. Similar phenomenon also happened in the conventional Co_3O_4 nanowires (Fig. S6).

It is considered that the CD measurement is more accurate than that of the CV measurement.[35] Thus, the specific capacitance of the Co_3O_4 nanowires@nanowires and conventional Co_3O_4 nanowires in this study were calculated based on their corresponding CD curves and the typical results are shown in Fig. 4e. The Co_3O_4 nanowires@nanowires possess high specific capacitances up to 1640, 1503, 1377, 1308, 1266, 1225, 1198, 1145, 1122 and 1083 F g^{-1} at 2, 4, 8, 12, 16, 20, 24, 32, 40 and 50 mA cm^{-2}, respectively, while the conventional Co_3O_4 nanowires only show specific capacitances of 560 and 298 F g^{-1} at 2 and 20 A g^{-1}, respectively. It is well accepted that the rate capability is a vital factor for the supercapacitors in high power applications. The decline of the specific capacitances along with the increase of current density may be ascribed to the incremental voltage drop and insufficient active material involved in redox reaction. As can be seen, the Co_3O_4 nanowires@nanowire electrode preserved 74.7% of its specific capacitance (from 1640 to 1225 F g^{-1}) with the current increasing from 2 to 20 mA cm^{-2}. However, the specific capacitance of the conventional Co_3O_4 nanowires can only preserved 53.2% under the same change interval of current density, much less than the Co_3O_4 nanowires@nanowire electrode material on the Ni foam. Furthermore, even at a higher current density of 50 mA cm^{-2}, the Co_3O_4 nanowires@nanowires still can preserved 66% of the specific capacitance at 2 mA cm^{-2}. The predominant specific capacitance of our sample is mainly due to its ability to have short paths for ion diffusion in the Co_3O_4 nanowire interconnected network, and sufficient utilization of active material due to its ultrafine microstructures.[36] It is noteworthy that both of the specific capacitance and rate capability reported here were remarkable compared with those pure Co_3O_4 as well as Co_3O_4-based hybrid electrode materials reported in previous literature,[18-20, 37-48] as summarized in Table S1.†

Fig. 4f shows the Ragone plot (power density vs. energy density) for the two electrodes at the potential window of 0-0.45 V. At a power density of 549 W kg^{-1}, the Co_3O_4 nanowires@nanowires delivered an energy density as high as 46.12 Wh kg^{-1}, which is almost 3 times larger than that of the conventional Co_3O_4 nanowires (15.76 Wh kg^{-1}). The energy density of the Co_3O_4 nanowires@nanowires electrode materials is higher than those of the reported nanostructured Co_3O_4 electrodes, such as Co_3O_4 nanowire arrays (31.68 Wh kg^{-1}),[49] hollow Co_3O_4 microspheres (34.51 Wh kg^{-1}),[50] multi-shelled Co_3O_4 hollow microspheres (13.7 Wh kg^{-1}), [51] mesoporous Co_3O_4 nanoflake arrays (18.91 Wh kg^{-1}),[52] 3D hierarchical mesoporous Co_3O_4 nanoparticles (15.24 Wh kg^{-1})[53] and 3D enoki mushroom-like Co_3O_4 hierarchitectures (22.13 Wh kg^{-1}).[54] More importantly, the energy density of the Co_3O_4 nanowires@nanowire electrode materials can still reach 30.46 Wh kg^{-1} even at a high power density of 13720 W kg^{-1}.

Nyquist plots of the two Co_3O_4 electrodes also were investigated and shown in Fig. 4g. The two impedance curves are similar in form, with an arc in the high-frequency region and a spike at lower frequencies. The inset of Fig. 4g shows the equivalent fitting circuit analysis of the as-synthesized Co_3O_4 electrodes using a complex nonlinear least-squares fitting method.[55] The equivalent series resistance (R_s) value of the Co_3O_4 nanowires@nanowires was only 0.26 Ω, which was lower than that (0.30 Ω) of the conventional Co_3O_4 nanowires. In particular, the Co_3O_4 nanowires@nanowires have a smaller charge transfer resistance (R_{ct}) value (2.93 Ω) than that of the conventional Co_3O_4 nanowires (4.54 Ω), which demonstrates that the unique microstructure can provide an ideal pathway for electron and ion transport without kinetic limitations. It is worth mentioning that the as-fitted equivalent circuits have higher accuracy as the as-obtained fitting curves of these two Co_3O_4 electrodes can match the original testing impedance curves very well, as shown in Fig. 4h. The durability of electrode material also is a critical factor except higher specific capacitance as well as superior rate capability for practical applications. The cycling stability of the Co_3O_4 nanowires@nanowires was measured by the repeated CV measurement at a scan rate of 50 mV s^{-1}, as shown in Fig. 4i. The final specific capacitance of the Co_3O_4 nanowires@nanowires is 99.03% of its initial value after 10000 cycles. There is a minor damage of the Co_3O_4 nanowires@nanowires electrode active materials after experiencing harsh and frequent phase variations during the redox reactions (shown in Fig. S7). The outstanding lifespan of the Co_3O_4 nanowires@nanowires electrode material were mainly ascribed to the unique core/shell structure consisting ultrafine nanowires which provides more active sites for efficient electrolyte ion transportation.

The above electrochemical measurements indicate that the unique hierarchical Co_3O_4 nanowires@nanowires can deliver fascinating electrochemical performance with high specific capacitance, superior rate capability as well as remarkable cycling stability synchronously. The outstanding electrochemical properties could be related to the following structural and morphological peculiarities. (i) Co_3O_4 is a kind of good super-capacitive metal oxide material and Co_3O_4 microstructures grown on the Ni foam directly could avoid "dead" volume caused by the tanglesome process of mixing active materials with binders and carbon powder; (ii) the reasonable room among the interconnected hierarchical crystalline nanounits possessing more electroactive sites allows for easy diffusion of the electrolyte into the inner region of the electrodes; (iii) The core (interior nanowires) can offer an efficient way of transporting the ions or electrons, while the shell (external ultrafine nanowires) can result in short paths for electron and ion transport as well as species diffusion. Thus, the as-obtained hierarchical Co_3O_4 nanowires@nanowires can engage in the reversible faradic reaction adequately and deliver fascinating electrochemical performance.

Conclusions

A facile, low-cost and effective hydrothermal process was developed to synthesize Co_3O_4 nanowires@Co_3O_4 ultrafine nanowires directly grown on the Ni foam with high electrochemical properties as a supercapacitor electrode. The as-synthesized Co_3O_4 hierarchical microstructure electrode on the Ni foam demonstrated excellent electrochemical performances with high specific capacitance (1640 F g^{-1} at 2 mA cm^{-2}), desirable rate capability (66% retention from 2 to 50 mA cm^{-2}) and superior long lifespan (99.03% of the initial value after 10000 cycles) simultaneously. Such a high electrochemical behavior can be attributed to the unique structural

and morphological peculiarities of the Co_3O_4 nanowires@Co_3O_4 ultrafine nanowires core/shell hierarchical microstructure. It is expected that the Co_3O_4 nanowires@Co_3O_4 ultrafine nanowires can be a promising electrode materials for the supercapacitor applications.

Acknowledgements

This work was financially supported by the National Natural Science Foundation of China (Grants 21171035, 51302035, 51472049, and 11204030), the Ph.D. Programs Foundation of the Ministry of Education of China (Grants 20110075110008 and 20130075120001), the National 863 Program of China (Grant 2013AA031903), and the Fundamental Research Funds for the Central Universities. The Key Grant Project of Chinese Ministry of Education (Grant 313015), the Science and Technology Commission of Shanghai Municipality (Grant 13ZR1451200), the Program Innovative Research Team in University (Grant IRT1221), the Hong Kong Scholars Program, the Shanghai Leading Academic Discipline Project (Grant B603), and the Program of Introducing Talents of Discipline to Universities (Grant 111-2-04)

Notes and references

[a] State Key Laboratory for Modification of Chemical Fibers and Polymer Materials, College of Materials Science and Engineering, Donghua University, Shanghai 201620, China.
[b] Ian Wark Research Institute, University of South Australia, Mawson Lakes, SA 5095, Australia.
[c] School of Fundamental Studies, Shanghai University of Engineering Science, Shanghai 201620, China.
[d] School of Material Engineering, Shanghai University of Engineering Science, Shanghai 201620, China.
[e] Center of Super-Diamond and Advanced Films (COSDAF), Department of Physics and Materials Science, City University of Hong Kong, Hong Kong.

E-mail: hu.junqing@dhu.edu.cn.

Electronic Supplementary Information (ESI) available. See DOI: 10.1039/b000000x/

1 J. R. Miller and P. Simon, *Science*, 2008, 321, 651.
2 G. Nystrom, A. Marais, E. Karabulut, L. Wagberg, Y. Cui and M. M. Hamedi, *Nat. Commun.*, 2015, 6, 7259.
3 N. S. Choi, Z. Chen, S. A. Freunberger, X. Ji, Y. K. Sun, K. Amine, G. Yushin, L. F. Nazar, J. Cho and P. G. Bruce, *Angew. Chem. Int. Ed.*, 2012, 51, 9994.
4 X. H. Lu; T. Y. Liu; Te. Zhai; G. M. Wang; M. H. Yu; S. L. Xie; Y. C. Ling; C. L. Liang; Y. X. Tong and Y. Li, *Adv. Energy Mater.*, 2014, 4, 1300994.
5 C. Guan, J. L. Liu, Y. D. Wang, L. Mao, Z. X. Fan, Z. X. Shen, H. Zhang and J. Wang, *ACS Nano*, 2015, 9, 5198.
6 D. Pech, M. Brunet, H. Durou, P. Huang, V. Mochalin and Y. Gogotsi, *Nat. Nanotechnol.*, 2010, 5, 651.
7 J. Jiang, Y. Li, J. Liu, X. Huang, C. Yuan and X. W. Lou, *Adv. Mater.*, 2012, 24, 5166.
8 C. Guan, X. L. Li, Z. L. Wang, X. H. Cao, C. Soci, H. Zhang and H. J. Fan, *Adv. Mater.*, 2012, 24, 4186.
9 G. H. Yu, L. B. Hu, M. Vosgueritchian, H. L. Wang, X. Xie, J. R. McDonough, X. Cui, Y. Cui and Z. N. Bao, *Nano Lett.*, 2011, 11, 2905.
10 W. B. Zhang, L. B. Kong, X. J. Ma, Y. C. Luo and L. Kang, *New J. Chem.*, 2014, 38, 3236.
11 R. B. Rakhi, W. Chen, D. K. Cha and H. N. Alshareef, *Nano Lett.*, 2012, 12, 2559.
12 G. X. Wang, X. P. Shen, J. Horvat, B. Wang, H. Liu, D. Wexler and J. Yao, *J. Phys. Chem. C*, 2009, 113, 4357.
13 T. Y. Wei, C. H. Chen, K. H. Chang, S. Y. Lu and C. C. Hu, *Chem. Mater.*, 2009, 21, 3228.
14 Y. H. Xiao, S. J. Liu, F. Li, A. Q. Zhang, J. H. Zhao, S. M. Fang and D. Z. Jia, *Adv. Funct. Mater.*, 2012, 22, 4052.
15 Q. Y. Liao, N. Li, S. X. Jin, G. W. Yang and C. X. Wang, *ACS Nano*, 2015, 9, 5310.
16 X. H. Xia, J. P. Tu, X. L. Wang, C. D. Gu and X. B. Zhao, *Chem. Commun.*, 2011, 47, 5786.
17 Y. T. Hao, H. W. Wang, Z. H. Hu, L. H. Gan and Z. J. Xu, *New J. Chem.*, 2015, 39, 68.
18 S. Vijayakumar, A. Kiruthika Ponnalagi, S. Nagamuthu and G. Muralidharan, *Electrochim. Acta*, 2013, 106, 500.
19 H. Pang, F. Gao, Q. Chen, R. M. Liu and Q. Y. Lu, *Dalton Trans.*, 2012, 41, 5862.
20 X. M. Liu, Q. Long, C. H. Jiang, B. B. Zhan, C. Li, S. J. Liu, Q. Zhao, W. Huang and X. C. Dong, *Nanoscale*, 2013, 5, 6525.
21 Y. Z. Zhang, Y. Wang, Y. L. Xie, T. Cheng, W. Y. Lai, H. Pang and W. Huang, *Nanoscale*, 2014, 6, 14354.
22 Y. J. Cao, W. Y. Li, K. B. Xu, Y. X. Zhang, T. Ji, R. J. Zou, J. M. Yang, Z. Y. Qin and J. Q. Hu, *J. Mater. Chem. A*, 2014, 2, 20723.
23 F. Z. Deng, L. Yu, G. Cheng, T. Lin, M. Sun, F. Ye and Y. F. Li, *J. Power Sources*, 2014, 251, 202.
24 L. Su, Y. Jing and Z. Zhou, *Nanoscale*, 2011, 3, 3967.
25 J. Duay, S. A. Sherrill, Z. Gui, E. Gillette and S. B. Lee, *ACS Nano*, 2013, 7, 1200.
26 X. H. Xia, J. P. Tu, Y. Q. Zhang, X. L.Wang, C. F. D. Gu, X. B. Zhao and H. J. Fan, *ACS Nano*, 2012, 6, 5531.
27 J. Jiang, J. P. Liu; X. T Huang, Y. Y. Li, R. M Ding, X. X. Ji, Y. Y. Hu, Q. B Chi and Z. H. Zhu, *Cryst. Growth Des.*, 2010, 10, 70.
28 X. Y. Liu, Y. Q. Zhang, X. H. Xia, S. J. Shi, Y. Lu, X. L. Wang, C. D. Gu and J. P. Tu, *J. Power Sources*, 2013, 239, 157.
29 W. Zhu, Z. Y. Lu, G. X. Zhang, X. D. Lei, Z. Chang, J. F. Liu and X. M. Sun, *J. Mater. Chem. A*, 2013, 1, 8327.
30 M. J. Deng, F. L. Huang, I. W. Sun, W. T. Tsai and J. K. Chang, *Nanotechnology*, 2009, 20, 175602.
31 C. W. Kung, H. W. Chen, C. Y. Lin, R. Vittal and K. C. Ho, *J. Power Sources*, 2012, 214, 91.
32 X. W. Lou, D. Deng, J. Y. Lee and L. A. Archer, *J. Mater. Chem.*, 2008, 18, 4397.
33 H. W. Shim, A. H. Lim, J. C. Kim, E. J. Jang, S. D. Seo, G. H. Lee, T. D. Kim and D. W. Kim, *Sci. Rep.*, 2013, 3, 2325.
34 H. T. Wang, L. Zhang, X. H. Tan, C. M. B. Holt, B. Zahiri, B. C. Olsen and D. Mitlin, *J. Phys. Chem. C*, 2011, 115, 17599.
35 L. Zhao, L. Z. Fan, M. Q. Zhou, H. Guan, S. Y. Qiao, M. Antonietti and M. M. Titirici, *Adv. Mater.*, 2010, 22, 5202.
36 H. Jiang, T. Zhao, J. Ma, C. Yan and C. Li, *Chem. Commun.*, 2011, 47, 1264.
37 W. Du, R. M. Liu, Y. W. Jiang, Q. Y. Lu, Y. Z. Fan, F. Gao, *Journal of Power Sources*, 2013, 227, 101.
38 X. Zhang, Y. Q. Zhao and C. L. Xu, *Nanoscale*, 2014, 6, 3638.

39 M. X. Liao, Y. F. Liu, Z. H. Hu and Q. Yu, *J Alloy Compd.*, 2013, 562, 106.
40 W. L. Yanga, Z. Gao, J. Ma, J. Wang, B. Wang and L. H. Liu, *Electrochim. Acta*, 2013, 112, 378.
41 K. Wang, Z. Q. Shi, Y. Y. Wang, Z. G. Ye, H. Y. Xia, G. W. Liu and G. J. Qiao, *J Alloy Compd.*, 2015, 624, 85.
42 K. W. Qiu, H. L. Yan, D. Y. Zhang, Y. Lu, J. B. Cheng, M. Lu, C. L. Wang, Y. H. Zhang, X. M. Liu and Y. S. Luo, *J. Solid. State. Electrochem.*, 2015, 19, 391.
43 J. P. Liu, J. Jiang, C. W. Cheng, H. X. Li, J. X. Zhang, H. Gong and H. J. Fan, *Adv. Mater.*, 2011, 23, 2076.
44 K. B. Wang, Z. Y. Zhang, X. B. Shi, H. J, Wang, Y. N. Lu and X. Y. Ma, *RSC Adv.*, 2015, 5, 1943.
45 D. P. Cai, H. Huang, D. D. Wang, B. Liu, L. L. Wang, Y. Liu, Q. H. Li and T. H. Wang, *ACS Appl. Mater. Interfaces*, 2014, 6, 15905.
46 L. B. Ma, H. Zhou, X. P. Shen, Q. R. Chen, G. X. Zhu and Z. Y. Ji, *RSC Adv.*, 2014, 4, 53180.
47 S. Balasubramanian and P. K. Kamaraj, *Electrochim. Acta*, 2015, 168, 50.
48 X. W. Wang, S. Q. Liu, H. Y. Wang, F. Y. Tu, D. Fang and Y. H. Li, *J. Solid. State. Electrochem.*, 2012, 16, 3593.
49 X H. Xia, J. P. Tu, Y. Q. Zhang, Y. J. Mai, X. L. Wang, C. D. Gu and X. B. Zhao, *RSC Adv.*, 2012, 2, 1835.
50 C. Feng, J. F. Zhang, Y. D. Deng, C. Zhong, L. Liu and W. B. Hu, *RSC Adv.*, 2015, 5, 42055.
51 Y. P. Wang, A. Q. Pan, Q. Y. Zhu, Z. W. Nie, Y. F. Zhang, Y. Tang, S, Q. Liang and G. Z. Cao, *J. Power Sources*, 2014, 272, 107.
52 A. G. Xiao, S. B. Zhou, C. G. Zuo, Y. B. Zhuan and X. Ding, *Mater. Res. Bull.*, 2014, 60, 674.
53 Y. F. Fan, G. J. Shao, Z. P. Ma, G. L. Wang, H. B. Shao and S. Yan, *Part. Part. Syst. Char.*, 2014, 31, 1079.
54 F. L. Luo, J. Li, Y. Lei, W. Yang, H. Y. Yuan and D. Xiao, *Electrochim. Acta*, 2014, 135, 495-502.
55 Z. Fan, J. Yan, T. Wei, L. Zhi, G. Ning, T. Li and F. Wei, *Adv. Funct. Mater.*, 2011, 21, 2366.

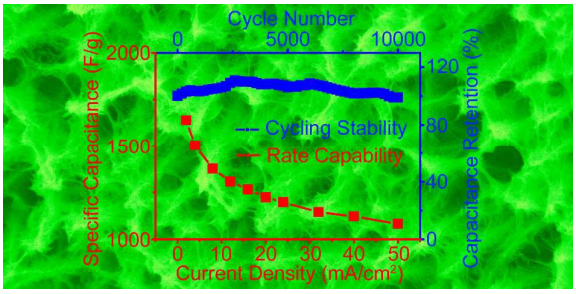

The hierarchical Co_3O_4 nanowires@Co_3O_4 ultrafine nanowires as an electrode delivered high specific capacitance, superior rate performance and long lifespan.